

Chapter 18

In Vivo ^1H -NMR Microimaging During Seed Imbibition, Germination, and Early Growth

Victor Terskikh, Kerstin Müller, Allison R. Kermode, and Gerhard Leubner-Metzger

Abstract

Magnetic resonance imaging (MRI) is a superior noninvasive diagnostic tool widely used in clinical medicine, with more than 60 million MRI tests performed each year worldwide. More specialized high-resolution MRI systems capable of a resolution that is 100–1,000 times higher than standard MRI instruments are used primarily in materials science, but are used with increasing frequency in plant physiology. We have shown that high-resolution ^1H -nuclear magnetic resonance (NMR) microimaging can provide a wealth of information about the internal anatomy of plant seeds as small as 1 mm or even smaller. This chapter covers the methods associated with these imaging techniques in detail. We also discuss the application of ^1H -NMR microimaging to study in vivo seed imbibition, germination, and early seedling growth.

Key words: Nuclear magnetic resonance, Magnetic resonance imaging, Microimaging, Chemical shift selective imaging, Seed imbibition, Germination

1. Introduction

Water uptake is a fundamental requirement for the initiation and completion of seed germination (1, 2). “Dry” orthodox seeds usually have water potentials between -350 and -50 MPa corresponding to a moisture content of only 5–10%. Water has by definition a water potential of 0 MPa, and leaf tissue has a water potential around -1 MPa. The water potential of plant tissues or of soil is determined by the sum of their pressure potential (a positive hydrostatic or turgor pressure), osmotic potential (a negative osmotic pressure), and matric potential (a negative value, important for “dry” states). Uptake of water by a “dry” seed is triphasic with a rapid initial uptake (phase I, i.e., imbibition) followed by a plateau

phase (phase II). A further increase in water uptake occurs only after germination is completed, as the embryo axis elongates after having emerged from all the seed-covering layers. Because dormant seeds do not complete germination, they do not enter this postgermination phase of water uptake (phase III). Abscisic acid (ABA) inhibits phase III water uptake and the transition from germination to postgerminative growth (3–5). While the temporal pattern of water uptake by seeds has been well-studied in different species, far less is known about its spatial distribution within seed tissues and how it is affected by plant hormones, environmental cues, and seed-covering layers/coats.

^1H -nuclear magnetic resonance (NMR) imaging (MRI) is a noninvasive in vivo technique that allows the acquisition of sequential cross-sectional two-dimensional (2D) and three-dimensional (3D) images of the spatial distribution of ^1H nuclei (mobile protons) and as such has been applied to plant biology (e.g., (3, 6–10)). The underlying principle of ^1H -NMR is that the ^1H nuclei carry a non-zero spin and, therefore, a magnetic moment. NMR signals occur if a sample with ^1H nuclei is immersed in a strong, external, static magnetic field (B_0) and is exposed to energy delivered by radio frequency pulses (11). The interaction of the magnetic moment with the field B_0 causes the nuclear spins to align and thus creates a small magnetization vector within the sample. The application of the radio frequency pulses of a given power and duration manipulates this magnetization. After the application of the radio frequency pulse, the magnetization vector spins around B_0 with its specific Larmor frequency, which is proportional to the field strength. For ^1H nuclei at a magnetic field strength B_0 of 9.4 T, the Larmor frequency is 400 MHz. NMR imaging is based on the fact that the Larmor frequency is proportional to the polarizing magnetic field. If in addition to B_0 a uniform magnetic field gradient G is applied, this frequency experiences a spatial signature and its position can be calculated. The interaction of the magnetic moment with externally applied magnetic field gradients and radio frequencies is used to obtain two-dimensional or three-dimensional images. In cases where the resolved volume elements are finer than the resolution of the unaided human eye (approx. 0.1 mm), this method of imaging may be termed microscopic or microimaging (12). A recent review by Stark et al. (11) further describes these techniques.

^1H -NMR imaging and microimaging have been used to study water uptake and flow during germination in relatively large seeds/fruits of angiosperms and gymnosperms, including those of legumes (13–16), conifers (17–19), cereal grains (11, 20–26), and others (27). Redistribution of water and tissue-specific differences in moisture content and water entry points were detected in these seeds. For example, in developing spruce (*Picea glauca*) seeds, water was concentrated at the radicle pole (17). In western white

pine (*Pinus monticola*) seeds, imbibition is characterized by water penetration through the seed coat and megagametophyte (18). The cotyledons of the embryo (located in the chalazal end of the seed) are the first to show hydration followed by the hypocotyl and later the radicle. After penetrating the seed coat, water in the micropylar end of the seed likely also contributes to further hydration of the embryo; however, the micropyle itself does not appear to be a site for water entry into the seed (18). The endosperm is a prominent structure in cereal caryopses, and it shows certain specific characteristics in the spatial pattern of water uptake. In cereal grains, the seed coat and the embryo–scutellum region appear to be barriers to water uptake by the embryo (21–24). Prior to the completion of germination, water must accumulate in the embryo–scutellum tissues for redistribution to the endosperm to take place. Delayed or protracted hydration severely limits germination. Dissection studies of cereal seeds show that the hydration properties of seed tissues differ and that the endosperm can act as a water reservoir under water-limiting conditions (22, 24).

MRI experiments with tobacco seeds illustrate how microimaging can be successfully applied to seeds smaller than 1 mm in size (3, 28). A time course analysis of tobacco seed germination exhibits a “two-step” pattern: testa rupture (Fig. 1, top) precedes endosperm rupture (Fig. 1, bottom), which is the visible completion of germination (radicle protrusion). NMR microimaging confirms that water distribution in phase II and phase III tobacco seeds is not homogeneous. The micropylar seed end, where endosperm rupture occurs, appears to be the major entry point of water. The micropylar endosperm and the radicle show the highest hydration.

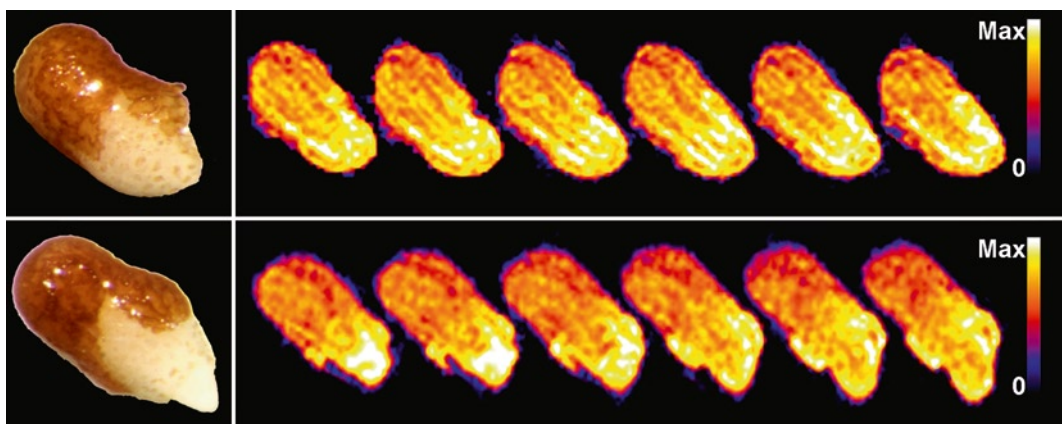


Fig. 1. Noninvasive in vivo ¹H-NMR microimaging of water uptake and distribution during tobacco seed germination. The spatial distribution of protons within the seed tissues is visualized with false colors as shown. The NMR microimages were obtained with 30 μ m spatial resolution. Also shown are corresponding microphotographs of seeds in the testa rupture (top left) and endosperm rupture (bottom left) stages. Modified from Manz et al. (3), <http://www.plantphysiol.org>, Copyright American Society of Plant Biologists.

This spatial pattern of water uptake is already evident during the early phase of imbibition before visible testa rupture. It becomes even more pronounced during testa rupture and remains pronounced after endosperm rupture. These results intimate that the radicle and the micropylar endosperm of the tobacco seed have enhanced water-holding capacities and can serve as a water reservoir for the embryo during germination. The inhibition by ABA of tobacco endosperm rupture and phase III water uptake does not appear to involve an effect of ABA on the spatial distribution of water in the seed. Testa rupture and initial embryo elongation cause an additional increase in water uptake in the second half of phase II. The additional increase in water content in the late part of phase II of water uptake is also evident in ABA-treated seeds, which supports the contention that initial embryo elongation and water uptake by the micropylar endosperm are not inhibited by ABA. Water uptake by dormant tobacco seeds (29) is likewise congruent. Germination of these seeds is blocked before testa rupture and there is no additional increase in water content in late phase II of water uptake. ABA, therefore, inhibits germination and phase III of water uptake by the emerging embryo, but it does not inhibit phase II water uptake needed for initial embryo elongation. Further, its inhibitory action is not mediated by reducing the water-holding capacity of the micropylar endosperm (3).

Overall, these studies are important for understanding the germination characteristics of seeds; different seed tissues and organs hydrate at different extents and show different spatial characteristics of water distribution, and the micropylar endosperm of some seeds, such as tobacco, acts as a water reservoir for the embryo.

Dry tobacco seeds contain approximately 43% of triacylglycerols (TAGs) per fresh weight as the most abundant nutrient storage reserve (3, 28). In oilseeds, like tobacco, the TAGs are stored in oil bodies and are genuinely liquid at room temperature, thus contributing to $^1\text{H-NMR}$ microimages due to high proton mobility. The MRI images of phase I tobacco seeds represent a combination of the spatial contents of TAGs and water. The proton mobility becomes essentially specific for water during phase II as in this phase the TAG peaks are very small compared to the water peak (see Note 1).

Since water and oil NMR signals are well-separated by their chemical shifts, it is possible to obtain separate water- or oil-specific MRI images using a chemical shift selective imaging (CSSI) technique as illustrated in Fig. 2 for western white pine seeds (also see ref. 18). In imbibed pine seeds, mobile water is mainly concentrated in the embryo and the seed coats while both the megagametophyte and the embryo show high concentrations of storage oils. $^1\text{H-NMR}$ CSSI microimages of a germinating seed clearly show that the initiation of postgerminative reserve mobilization across the megagametophyte storage tissue and the embryo exhibits

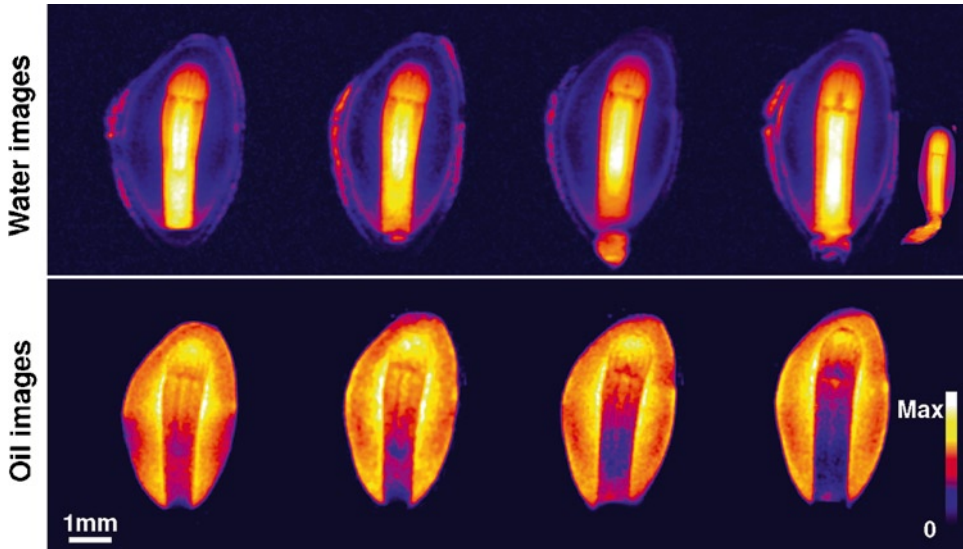


Fig. 2. In vivo ^1H -NMR chemical shift selective imaging (CSSI) of western white pine seed during germination. The spatial distribution of water (*upper row*) and oil (*lower row*) simultaneously mapped in the same seed over a course of early germination (*left to right*) is visualized with false colors as shown. Coronal plane 2D MRI images were obtained with a $78\ \mu\text{m}$ in-plane resolution and a $500\text{-}\mu\text{m}$ slice thickness. For more information on experimental details, see ref. 18.

distinct regional (i.e., spatial) differences. Mobilization of the major lipid storage reserves commences first within the meristematic region of the embryo and is likely important for early seedling establishment (Fig. 2). In the megagametophyte (which generally comprises the bulk of the seed), the oil mobilization commences only after radicle and cotyledon elongation/expansion, i.e., it is a postgerminative event. Thus, the chemical shift selective ^1H -NMR microimaging allows direct in vivo monitoring of oil reserve mobilization during early postgerminative growth, a process upon which seedling emergence depends.

2. Materials

1. Seeds of *Nicotiana tabacum* (tobacco), *Pinus monticola* (western white pine), or other species.
2. Autoclaved distilled water or a weak salt medium, e.g., 1/10 Murashige and Skoog (MS) salts without organic additions (4).
3. Plastic Petri dishes, filter paper, and a growth chamber or incubator that can be maintained at a constant temperature and light intensity.
4. Bruker Avance 400 NMR spectrometer (Bruker, Rheinstetten, Germany) with a vertical 9.4 T magnet and a proton resonance

frequency of 400 MHz (8, 30) as per the NMR experiments conducted on tobacco seeds (3).

5. Bruker Avance DRX 360 spectrometer equipped with a Bruker 2.5 microimaging system as per the NMR experiments conducted on pine seeds (18).

3. Methods

3.1. Seed Germination

1. Tobacco seeds are sown in plastic Petri dishes containing filter paper wetted with water and incubated at a constant temperature around 20°C in continuous white light. Other species may require different germination temperatures and a previous dormancy-breaking treatment.
2. Dry seeds of western white pine (*Pinus monticola* Dougl. ex D. Don) and dry seeds are first soaked in running water at 23°C for 12 days prior to subjecting them to a subsequent prolonged moist-chilling treatment as described in Chapter 4 and in (31). Germination conditions are also described in (31).
3. The seeds are sampled after different time periods after imbibition of dry seeds (tobacco) or after seeds have been transferred into germination conditions after dormancy breakage (western white pine). The time course of germination must be monitored. For example, for tobacco seeds, one scores the percentage of testa and endosperm rupture over time in order to correlate the ¹H-NMR microimaging results with defined seed stages during germination (Fig. 1) (see Note 2).

3.2. In Vivo ¹H-MAS NMR Spectroscopic Analyses of Seed Moisture

1. For magnetic angle spinning (MAS) NMR spectroscopy, the intact seeds (dry seeds or seeds sampled after imbibition) are placed inside a standard 4-mm MAS o.d. rotor (3). The rotation rate is set to 10 kHz, which has no influence on the seed morphology; due to the small rotor diameter, the centrifugal forces are low. Also see Chapter 17.
2. The peak areas below the water signals at 4.8 ppm are quantified, and the relative moisture contents per seed are calculated as described in (3).
3. For comparison, gravimetric determination of seed moisture contents in mg of water per seed can be obtained. For this, the samples are weighed before and after heating for 3 h at 100°C as described in (32).

3.3. In Vivo ¹H-NMR Microimaging

1. Intact seeds are placed inside a fitting glass capillary, e.g., 1.5 mm in diameter for tobacco (3), and, in order to avoid movement during the experiment, are pressed slightly against

each other with a piece of matching Teflon tube at each end of the glass tube (see Note 3).

2. The capillary secured in an MRI probe, which is then positioned inside the superconducting magnet. There is no external movement of the sample tube similar to the slow spinning used in high-resolution NMR spectroscopy.
3. MRI images of the proton density are acquired with a Bruker Micro2.5 microimaging hardware setup using a standard three-dimensional spin-echo pulse sequence employing echo times (TE) of 1 ms, recycle delays (TR) of 0.8 s, spectral width of 100 kHz, and an isotropic spatial resolution of $30 \times 30 \times 30 \mu\text{m}^3$.
4. Each image consists of $128 \times 64 \times 64$ data points, and at least two signal averages should be taken. The total acquisition time is 110 min per image for tobacco seeds (3) (see Note 4).
5. The experimental MRI conditions may vary depending on the seed size and the spatial resolution required. For example, for larger seeds, two-dimensional MRI images can be acquired with a slice thickness of 0.2–0.5 mm.
6. CSSI can be conducted with a broadline imaging package (BLIP) developed by Bruker which allows simultaneous acquisition of both water and oil images. In CSSI experiments, refocusing and selection pulses are 1.2 and 0.3 μs , respectively, with an echo time (TE) of 4–8 μs and a recycle delay (TR) of 1 s.
7. False-color images of slices can be obtained from raw data with image processing software, such as ImageJ, a public domain Java-based program (<http://rsb.info.nih.gov/ij/>).

4. Notes

1. In oil seeds, like tobacco, the ¹H-NMR signal of “dry” seeds and of seeds during phase I water uptake (imbibition) is due to oil and water. In phase II, the water peak becomes prominent and what is detected is essentially water (see Fig. 1 of Manz et al. (3)). Separate MRI images of oil and water can be acquired using CSSI (Fig. 2) (18).
2. To obtain meaningful results from an in vivo ¹H-NMR microimaging experiment, images must be obtained for several seeds at the same stages. Representative typical images may then be selected for presentation.
3. When several phase III seeds are placed together in the capillary for ¹H-NMR microimaging, the subsequent computer separation can become problematic because of overlaps in the growing structures. This is not a problem with phase II seeds.

4. Small seeds require higher resolution and this means longer acquisition times. If acquisition times exceed several hours, the physiological changes in the seed need to be taken into account.

Acknowledgments

This work is funded by a “Deutsche Forschungsgemeinschaft” (DFG LE720/6) grant awarded to G. Leubner-Metzger and a Natural Sciences and Engineering Research Council of Canada (NSERC) Strategic grant to A. Kermode and others. We are grateful for the use of NMR Facilities at the Fraunhofer Institute of Biomedical Engineering (IBMT), St. Ingbert, Germany and at the Plant Biotechnology Institute NRC, Saskatoon, SK, Canada.

References

1. Finch-Savage WE and Leubner-Metzger G (2006) Seed dormancy and the control of germination. *New Phytol.* **171**, 501–23.
2. Obroucheva NV and Antipova OV (1997) Physiology of the initiation of seed germination. *Russian J. Plant Physiol.* **44**, 250–64.
3. Manz B, Müller K, Kucera B, Volke F, and Leubner-Metzger G (2005) Water uptake and distribution in germinating tobacco seeds investigated *in vivo* by nuclear magnetic resonance imaging. *Plant Physiol.* **138**, 1538–51.
4. Müller K, Tintelnot S, and Leubner-Metzger G (2006) Endosperm-limited Brassicaceae seed germination: Abscisic acid inhibits embryo-induced endosperm weakening of *Lepidium sativum* (cress) and endosperm rupture of cress and *Arabidopsis thaliana*. *Plant Cell Physiol.* **47**, 864–877.
5. Schopfer P and Plachy C (1984) Control of seed germination by abscisic acid. II. Effect on embryo water uptake in *Brassica napus* L. *Plant Physiol.* **76**, 155–160.
6. MacFall JS and van As H (1996) Magnetic resonance imaging of plants. In: Shachar-Hill Y and Pfeffer PE, (eds). *Nuclear magnetic resonance in plant biology*. American Society of Plant Biologists, Rockville, Maryland, pp. 33–76.
7. Ratcliffe RG, *In vivo NMR spectroscopy: Biochemical and physiological applications to plants*, in *Nuclear magnetic resonance in plant biology*, Shachar-Hill Y and Pfeffer PE, Editors. 1996, American Society of Plant Biologists: Rockville, Maryland, U.S.A. p. 1–32.
8. Schneider H, Manz B, Westhoff M, Mimietz S, Szimtenings M, Neuberger T, Faber C, Krohne G, Haase A, Volke F, and Zimmermann U (2003) The impact of lipid distribution, composition and mobility on xylem water refilling of the resurrection plant *Myrothamnus flabellifolia*. *New Phytol.* **159**, 487–505.
9. Stark M, Manz B, Riemann I, Volke F, Weschke W, and König K (2007) Multiphoton and magnetic resonance imaging of Barley embryos: comparing micro-imaging techniques across scale and parameter barriers. *Proc SPIE* **6442**, 644227.
10. Van As H (2007) Intact plant MRI for the study of cell water relations, membrane permeability, cell-to-cell and long-distance water transport. *J. Exptl Bot.* **58**, 743–756.
11. Stark M, Manz B, Ehlers A, Küppers M, Riemann I, Volke F, Siebert U, Weschke W, and König K (2007) Multiparametric high-resolution imaging of barley embryos by multiphoton microscopy and magnetic resonance micro-imaging. *Microscopy Research and Technique* **70**, 426–432.
12. Callaghan PT, *Principles of nuclear magnetic resonance microscopy*. 1991, Oxford: Clarendon Press.
13. Poulliquen D, Gross D, Lehmann V, Ducournau S, Demilly D, and Lechappe J (1997) Study of water and oil bodies in seeds by nuclear magnetic resonance. *C R Acad Sci [iii]* **320**, 131–138.
14. Kikuchi K, Koizumi M, Ishida N, and Kano H (2006) Water uptake by dry beans observed by

- micro-magnetic resonance imaging. *Ann. Bot.* **98**, 545–53.
15. Koizumi M, Kikuchi K, Isobe S, Ishida N, Naito S, and Kano H (2008) Role of seed coat in imbibing soybean seeds observed by micro-magnetic resonance imaging. *Ann. Bot.* **102**, 343–52.
 16. Garnczarska M, Zalewski T, and Kempka M (2007) Water uptake and distribution in germinating lupine seeds studied by magnetic resonance imaging and NMR spectroscopy. *Physiol. Plant.* **130**, 23–32.
 17. Carrier DJ, Kendall EJ, Bock CA, Cunningham JE, and Dunstan DI (1999) Water content, lipid deposition, and (+)-abscisic acid content in developing white spruce seeds. *J. Exp. Bot.* **50**, 1359–1364.
 18. Terskikh VV, Feurtado JA, Ren C, Abrams SR, and Kermod AR (2005) Water uptake and oil distribution during imbibition of seeds of western pine (*Pinus monticola* Dougl. ex D. Don) monitored in vivo using magnetic resonance imaging. *Planta* **221**, 17–27.
 19. Terskikh VV, Zeng Y, Feurtado JA, Giblin M, Abrams SR, and Kermod AR (2008) Deterioration of western redcedar (*Thuja plicata* Donn ex D. Don) seeds: protein oxidation and in vivo NMR monitoring of storage oils. *J. Exp. Bot.* **59**, 765–777.
 20. Jenner CF, Xia Y, Eccles CD, and Callaghan PT (1988) Circulation of water within wheat grain revealed by nuclear magnetic resonance micro-imaging. *Nature* **336**, 399–402.
 21. Gruwel MLH, Yin XS, Edney MJ, Schroeder SW, MacGregor AW, and Abrams S (2002) Barley viability during storage: Use of magnetic resonance as a potential tool to study viability loss. *J. Agr. Food Chem.* **50**, 667–676.
 22. Allen PS, Thorne ET, Gardner JS, and White DB (2000) Is the barley endosperm a water reservoir for the embryo when germinating seeds are dried? *Int. J. Plant Sci.* **161**, 195–201.
 23. Hou JQ, Kendall EJ, and Simpson GM (1997) Water uptake and distribution in non-dormant and dormant wild oat (*Avena fatua* L.) caryopses. *J. Exp. Bot.* **48**, 683–692.
 24. Seefeldt HF, van den Berg F, Köckenberger W, and Engelsens SB (2007) Water mobility in the endosperm of high beta-glucan barley mutants as studied by nuclear magnetic resonance imaging. *Magn. Reson. Imaging* **25**, 425–432.
 25. Ishida N, Naito S, and Kano H (2004) Loss of moisture from harvested rice seeds on MRI. *Magn. Reson. Imaging* **22**, 871–5.
 26. Rathjen J, Strounina E, and Mares D (2009) Water movement into dormant and non-dormant wheat (*Triticum aestivum* L.) grains. *J. Exp. Bot.* **60**, 1619–1631.
 27. Roh MS, Bentz J-A, Wang P, Li E, and Koshioka M (2004) Maturity and temperature stratification affect the germination of *Styrax japonicus* seeds. *J. Hort. Sci. Biotechnol.* **79**, 645–651.
 28. Leubner-Metzger G (2005) β -1,3-Glucanase gene expression in low-hydrated seeds as a mechanism for dormancy release during tobacco after-ripening. *Plant J.* **41**, 133–145.
 29. Mohapatra SC and Johnson WH (1978) Development of the tobacco seedling. I. Relationship between moisture uptake and light sensitivity during seed germination in a flue-cured variety. *Tobacco Res.* **4**, 41–49.
 30. Manz B, Volke F, Goll D, and Horn H (2003) Measuring local flow velocities and biofilm structure in biofilm systems with magnetic resonance imaging (MRI). *Biotechnol. Bioeng.* **84**, 424–432.
 31. Terskikh VV, Feurtado JA, Borchardt S, Giblin M, Abrams SR, and Kermod AR (2005) *In vivo* ¹³C NMR metabolite profiling: potential for understanding and assessing conifer seed quality. *J. Exptl. Bot.* **56**, 2253–65.
 32. Leubner-Metzger G (2002) Seed after-ripening and over-expression of class I β -1,3-glucanase confer maternal effects on tobacco testa rupture and dormancy release. *Planta* **215**, 959–968.